Journal for ImmunoTherapy of Cancer

Hsa-LINC02418/mmu-4930573I07Rik regulated by METTL3 dictates anti-PD-L1 immunotherapeutic efficacy via enhancement of Trim21-mediated PD-L1 ubiquitination

Zhijia Sun,[1,2] Haixing Mai,[3] Chunyuan Xue,[1] Zhongyi Fan,[4] Jiangbo Li,[5] Hairui Chen,[3] Nan Huo,[1] Xiaofeng Kang,[1] Chuanhao Tang,[1] Liaoxin Fang,[1] Hui Zhao,[6] Yuchen Han,[1] Chao Sun,[1] Huanyan Peng,[1] Yimeng Du,[1] Jing Yang,[7] Nan Du,[6] Xiaojie Xu [1]

To cite: Sun Z, Mai H, Xue C, *et al*. Hsa-LINC02418/mmu-4930573I07Rik regulated by METTL3 dictates anti-PD-L1 immunotherapeutic efficacy via enhancement of Trim21-mediated PD-L1 ubiquitination. *Journal for ImmunoTherapy of Cancer* 2023;**11**:e007415. doi:10.1136/jitc-2023-007415

► Additional supplemental material is published online only. To view, please visit the journal online (http://dx.doi.org/10.1136/jitc-2023-007415).

ZS, HM, CX, ZF and JL contributed equally.

Accepted 10 November 2023

For numbered affiliations see end of article.

Correspondence to
Professor Xiaojie Xu; miraclexxj@126.com

Professor Nan Du; dunan05@aliyun.com

Professor Jing Yang; yangjing_301@126.com

Dr Yimeng Du; duyimeng1987@163.com

ABSTRACT

Background Limited response to programmed death ligand-1 (PD-L1)/programmed death 1 (PD-1) immunotherapy is a major hindrance of checkpoint immunotherapy in non-small cell lung cancer (NSCLC). The abundance of PD-L1 on the tumor cell surface is crucial for the responsiveness of PD-1/PD-L1 immunotherapy. However, the negative control of PD-L1 expression and the physiological significance of the PD-L1 inhibition in NSCLC immunotherapy remain obscure.

Methods Bioinformatics analysis was performed to profile and investigate the long non-coding RNAs that negatively correlated with PD-L1 expression and positively correlated with CD8+T cell infiltration in NSCLC. Immunofluorescence, *in vitro* PD-1 binding assay, T cell-induced apoptosis assays and *in vivo* syngeneic mouse models were used to investigate the functional roles of LINC02418 and mmu-4930573I07Rik in regulating anti-PD-L1 therapeutic efficacy in NSCLC. The molecular mechanism of LINC02418-enhanced PD-L1 downregulation was explored by immunoprecipitation, RNA immunoprecipitation (RIP), and ubiquitination assays. RIP, luciferase reporter, and messenger RNA degradation assays were used to investigate the m6A modification of LINC02418 or mmu-4930573I07Rik expression. Bioinformatics analysis and immunohistochemistry (IHC) verification were performed to determine the significance of LINC02418, PD-L1 expression and CD8+T cell infiltration.

Results LINC02418 is a negative regulator of PD-L1 expression that positively correlated with CD8+T cell infiltration, predicting favorable clinical outcomes for patients with NSCLC. LINC02418 downregulates PD-L1 expression by enhancing PD-L1 ubiquitination mediated by E3 ligase Trim21. Both hsa-LINC02418 and mmu-4930573I07Rik (its homologous RNA in mice) regulate PD-L1 therapeutic efficacy in NSCLC via Trim21, inducing T cell-induced apoptosis *in vitro* and *in vivo*. Furthermore, METTL3 inhibition via N6-methyladenosine (m6A) modification mediated by YTHDF2 reader upregulates hsa-LINC02418 and mmu-4930573I07Rik. In patients

WHAT IS ALREADY KNOWN ON THIS TOPIC

⇒ Understanding the underlying mechanisms of programmed death ligand-1 (PD-L1) regulation in non-small cell lung cancer (NSCLC) is helpful for improving the clinical benefit of programmed death 1 (PD-1)/PD-L1 blockade therapy. However, how the expression of PD-L1 is tightly controlled still remains elusive. Currently reported long non-coding RNAs (lncRNAs) are positive regulators of PD-L1 expression. However, lncRNAs that negatively regulate PD-L1 expression and their biological implications in response to PD-1/PD-L1 blockade therapy in NSCLC remain unclear.

WHAT THIS STUDY ADDS

⇒ LINC02418 functions as a newly discovered upstream negative regulator of PD-L1, enhancing the response to PD-L1 immunotherapy through its interaction with Trim21.

⇒ In NSCLC samples, the expression of LINC02418 was negatively correlated with PD-L1 expression and positively correlated with CD8+T cell infiltration.

⇒ These mechanisms elucidate the potential benefits of incorporating LINC02418 or Trim21 to enhance the therapeutic sensitivity of PD-1/PD-L1 blockade.

HOW THIS STUDY MIGHT AFFECT RESEARCH, PRACTICE OR POLICY

⇒ This study highlights the crucial role of LINC02418 in immune evasion in NSCLC.

⇒ This study highlights the importance of LINC02418, which exerts synergistic effects with PD-L1 monoclonal antibody (mAb) to promote T-cell killing in tumors, indicating a favorable clinical prognosis and offering potential implications for clinical tumor treatment.

with NSCLC, LINC02418 expression is inversely correlated with PD-L1 expression and positively correlated with CD8+T infiltration.

Conclusion LINC02418 functions as a negative regulator of PD-L1 expression in NSCLC cells by promoting the degradation of PD-L1 through the ubiquitin-proteasome pathway. The expression of LINC02418 is regulated by METTL3/YTHDF2-mediated m6A modification. This study illuminates the underlying mechanisms of PD-L1 negative regulation and presents a promising target for improving the effectiveness of anti-PD-L1 therapy in NSCLC.

BACKGROUND

Lung cancer is one of the most common malignancies and the main cause of cancer mortality around the world. Non-small cell lung cancer (NSCLC) accounts for the majority of lung cancer cases, a large number of which are diagnosed at the advanced stage, indicating therapeutic difficulty and poor prognosis.[1] In recent years, immune checkpoint inhibitors have revolutionized the treatment landscape and greatly improved outcomes for numerous malignancies including NSCLC.[2 3] Programmed death 1 (PD-1) is a crucial immune checkpoint in NSCLC. It is found on the surface of T cells and interacts with programmed cell death ligand 1 (PD-L1), which is commonly present on tumor cells. This interaction generates an inhibitory signal that suppresses T-cell responses, facilitating the evasion of tumor cells.[4] Blockade of the PD-1/PD-L1 interaction enhances the immune recognition and T-cell attack to tumor cells, exhibiting tremendously improved clinical outcome for the treatment of advanced NSCLC. However, a substantial proportion of patients fail to respond to PD-1/PD-L1 blockade therapy initially and many primary responders relapse over time, leading to limited clinical application and treatment failure.[5 6] The expression of PD-L1 has been suggested to be one of the critical factors for the applicability of PD-1/PD-L1 blockade.[7 8] Thus, understanding the underlying mechanisms of PD-L1 regulation in NSCLC is helpful for improving the clinical benefit of PD-1/PD-L1 blockade therapy. However, how the expression of PD-L1 is tightly controlled still remains elusive.

Long non-coding RNA (lncRNA) is a major class of non-coding RNAs with a length of more than 200 nt.[9] LncRNAs exert their functions by regulating gene expression in epigenetic modulation, transcription (or post-transcription), and translation.[10 11] Accumulating evidence has confirmed the roles of lncRNAs in regulating PD-L1 expression in NSCLC. Wei *et al* demonstrated that in NSCLC tissues, MALAT1 upregulates the expression of PD-L1 by controlling the miR-200a-3p/PD-L1 axis.[12] Chen *et al* demonstrated that the lncRNA SOX2-OT upregulates PD-L1 expression through the mammalian target of rapamycin (mTOR) signaling pathway, promoting the progression and immune escape of NSCLC cells.[13] However, currently reported lncRNAs are positive regulators of PD-L1 expression. To the best of our knowledge, lncRNAs that negatively regulate PD-L1 expression and their biological implications in response to PD-1/PD-L1 blockade therapy in NSCLC remain unclear.

Accumulating evidences have suggested that m6A modification, one of the major post-transcriptional modifications of eukaryotic RNAs, participates in various aspects of RNA homeostasis.[14] Importantly, dysregulated m6A profiles have been implicated in the carcinogenesis and progression as well as treatment resistance of NSCLC cells. However, the function of m6A modification and the role of m6A-modified lncRNAs in regulating the anti-tumor immunity of NSCLC remain elusive.

In this study, we screen and characterize an lncRNA named LINC02418 that negatively regulates PD-L1 expression and positively correlates with CD8+T cell infiltration in NSCLC, which is associated with good clinical outcomes. By enhancing the interaction between E3 ligase Trim21 and PD-L1, LINC02418 contributes to PD-L1 protein degradation, thereby downregulating PD-L1 expression. The LINC02418-Trim21-PD-L1 axis regulates immunotherapeutic resistance in NSCLC by inducing the T-cell induced apoptosis. Additionally, hsa-LINC02418 and its homologous RNA in mouse, mmu-4930573I07Rik, can be m6A methylated by METTL3 and triggered for degradation by YTHDF2. In patients with NSCLC, LINC02418 expression is negatively correlated with PD-L1 expression but positively correlated with CD8+T cell infiltration. Our work provides a novel negative regulator of PD-L1 and its mechanism of immune escape in NSCLC, identifying a promising new pharmaceutical intervention target for patients with NSCLC receiving anti-PD-L1 treatment.

MATERIALS AND METHODS

Cell lines

Human lung cancer cell lines (A549, H1703, H226) and Lewis lung carcinoma cells (LLCs) were obtained from American Type Culture Collection. Human lung cancer cell line PC-9 was purchased from Procell Biotechnology Company (Wuhan, China). Peripheral blood mononuclear cells (PBMCs) were isolated from the peripheral blood of healthy laboratory workers. A549 cells and LLCs were cultured in dulbecco's modified eagle's medium (DMEM) containing 10% fetal bovine serum (FBS). PC-9, H226, H1703 cells and PBMCs were maintained in RPMI-1640 medium supplemented with 10% FBS. All cells were incubated in a 37°C incubator under 5% CO_2.

Mouse model and immunoassay

The mouse model of lung cancer was generated using male C57BL/6 mice (aged 6–8 weeks, body weight 18–22 g). Mice were randomly divided into two groups. A total of 2×10^6 LLCs carrying mmu-4930573I07Rik vector or empty vector were subcutaneously injected into the right flank of mice. On day 7 after implantation, the mice were pooled and each group was further randomly subdivided into control and treatment group which were intraperitoneally injected with IgG2b or PD-L1 mAb (5 mg/kg) every 3 days, respectively. Tumor sizes were measured every 3 days and tumor volumes were calculated according to the following formula: volume=(length×width^2/2).[15] For

the survival study, the mice were monitored with tumor volume and mice were euthanized when tumor volume exceeded 1,200 mm^3. The experiment was terminated on the 50th day and the mice carrying tumors smaller than 1,200 mm^3 were considered as survivors. Statistical analysis was conducted using GraphPad Prism. Kaplan-Meier curves and the corresponding Gehan-Breslow-Wilcoxon tests were used to evaluate statistical differences between groups in the survival studies. All the animal experiments were approved and guided by the Ethics Committee of Beijing Institute of Biotechnology (approval number IACUC-DWZX-2022–009) and were performed following the 3Rs' recommendations (Reduction, Refinement and Replacement).

Analysis of TCGA and GEO data set

The NSCLC transcriptome data can be downloaded from the cancer genome atlas (TCGA) database. Differential gene analysis between high-CD274 and low-CD274 expression groups was performed using the limma package. After data sorting and merging, the expression matrices of messenger RNA (mRNA) and lncRNA were extracted. Heatmaps were drawn using the heatmap package. The mRNA expression matrix was scored for immune cells by using the CIBERSORT algorithm.[16] Weighted correlation network analysis (WGCNA) analysis of NSCLC immune cells was performed by combining the gene expression matrix of lncRNA and the immune cell score of each sample. Cluster and modular analysis were performed for each gene, and Pearson correlation coefficients were calculated for all modules and immune cells. The TOM heatmap was plotted for the module genes. The CERNA network mapping was performed using Cytoscape.

Lung adenocarcinoma and transcriptome expression data were downloaded from the TCGA database, with a total of 579 samples. According to the expression of Trim21, they were divided into high expression group and low expression group. Based on the LINC02418 expression, they were subdivided into a high expression group and a low expression group. The ratio of immune cell infiltration in the high and low expression groups was calculated using the CIBESORT algorithm.

Statistical analysis

SPSS V.23.0 and Prism V.8.0 (GraphPad) were used to analyze all experiment data. Quantitative data was presented as mean±SD and compared by using Student's t-test. Rates were compared by using the χ^2. The Pearson correlation coefficient was used for multivariate correlation analysis. All *in vitro* tests were repeated at least three times. P value<0.05 is considered statistically significant.

RESULTS

Identification and characterization of a novel lncRNA positively correlates with CD8+ T-cell infiltration and predicts good prognosis in NSCLC

To identify lncRNAs that negatively regulate PD-L1 expression, we divided PD-L1 expression into high and low groups and analyzed the differentially expressed genes between the two groups using the TCGA lung adenocarcinoma (LUAD) and lung squamous cell carcinoma (LUSC) data set, which contained 932 NSCLC tissues and 92 adjacent non-tumorous tissues (figure 1A). By applying the criteria (|logFC|>1, p<0.05), we identified 908 dysregulated genes in the high-CD274 and low-CD274 (PD-L1) expression groups, with the top 100 dysregulated genes being displayed in the heatmap (figure 1B). Among these dysregulated genes, 388 were downregulated in the PD-L1 high expression group, suggesting their potential to negatively regulate PD-L1. To further screen candidate lncRNAs regulating tumor immunology, we analyzed immune infiltration scores of mRNA expression profiles using CIBERSORT. Then, we used the resulting immune infiltration scores and lncRNA expression profiles to build correlation modules using WGCNA analysis (figure 1C). Twelve modules were identified when the DissThres was set as 0.25 after merging dynamic modules, with the salmon module found to exhibit a significantly positive correlation with CD8+ infiltration score (Pearson=0.76, p=0.01) (figure 1D). By taking the intersection of the 80 hub lncRNAs identified from the salmon module and the preliminarily identified 388 genes that are negatively associated PD-L1, two candidate lncRNAs (LINC02418 and H19) were screened out (figure 1E). Kaplan-Meier survival analysis further demonstrated that LINC02418 rather than H19 had clinical prognostic significance in NSCLC (online supplemental figure S1). Patients with a higher expression level of LINC02418 had better overall survival (OS) and recurrence-free survival (RFS) in both LUAD and LUSC (figure 1F), indicating that LINC02418 could potentially be a predictor for better NSCLC prognosis.

Subsequently, a bioinformatics network analysis confirmed the potential link between LINC02418 and CD274 (PD-L1), with CD274 (PD-L1) ranked as one of the top 10 genes with the strongest association with LINC02418 (figure 1G). To confirm the exact role of LINC02418 in NSCLC, we assessed the expression levels of PD-L1 and LINC02418 in four NSCLC cell lines (A549, PC-9, H226, H1703) (figure 1H). Interestingly, we found that endogenous PD-L1 level and LINC02418 level were negatively correlated. We chose the H1703 cell line, expressing LINC02418 at the lowest level, and the A549 cell line, expressing LINC02418 at a relatively high level, for LINC02418 overexpression and knockdown experiments, respectively. Our results indicated that overexpression of LINC02418 markedly decreased PD-L1 expression in H1703 cells, while knockdown of LINC02418 with the specific smart pool of silencers increased the expression of PD-L1 in A549 cells (figure 1I). These data collectively

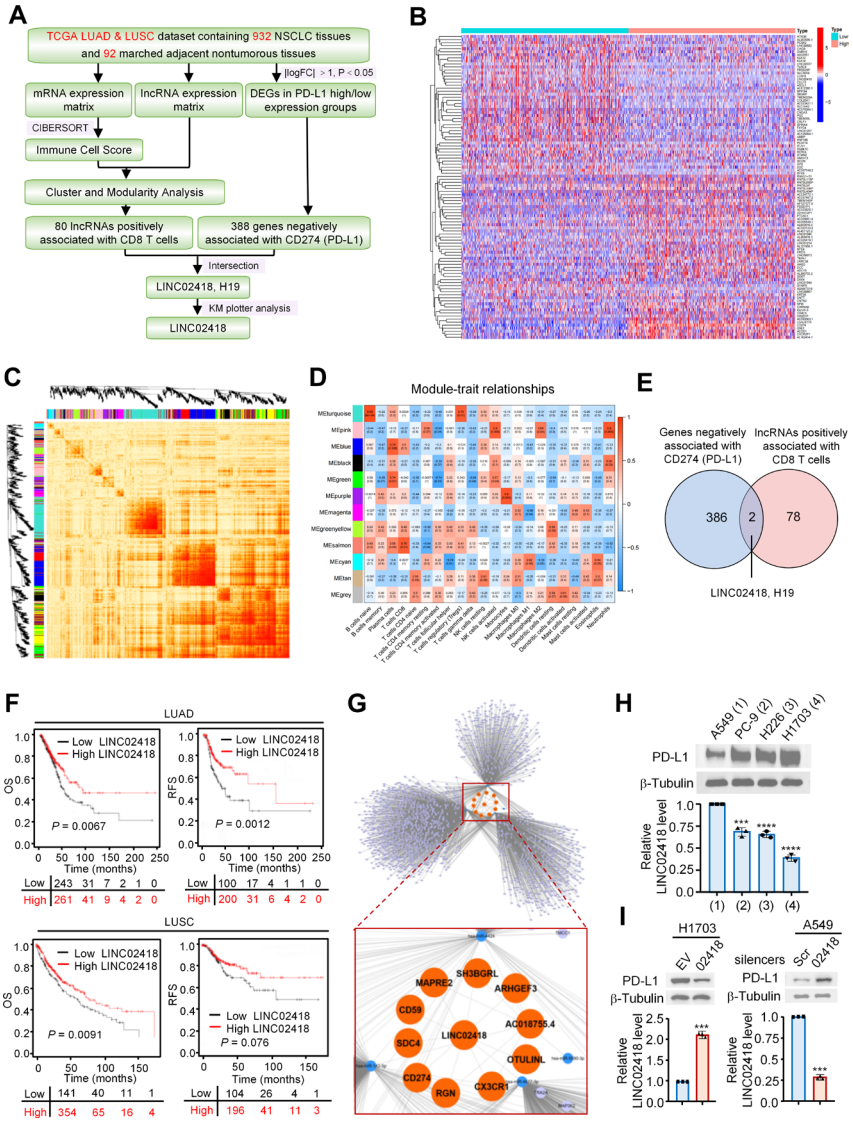

Figure 1 Identification and characterization of a novel lncRNA positively correlates with CD8+T cell infiltration and predicts a good prognosis in NSCLC. (A) Schematic diagram of the screening process. (B) Heatmap of the top 100 dysregulated lncRNAs in the high-CD274 and low-CD274 (PD-L1) expression groups. (C) The TOM heatmap shows the module genes obtained by WGCNA analysis combining the lncRNA expression matrix and the immune cell score. (D) The heatmap shows the correlation between the module genes of lncRNA and immune cells, with the upper number in each module represents the Pearson coefficient and the lower number represents the p value. (E) Venn diagram shows the intersected genes that are negatively associated with CD274 and positively associated with CD8+T cells. (F) Kaplan-Meier analysis of the overall survival (OS) rate and recurrence-free survival (RFS) rate of patients with NSCLC with low or high expression of LINC02418 (http://kmplot.com/analysis). Low or high LINC02418 expression was grouped by choosing the auto select best cut-off option. (G) Network analysis of the lncRNA (LINC02418), mRNAs, and miRNAs intersection in (A). The orange circles represent LINC02418 and the top 10 mRNAs with the highest correlation coefficient, the light blue circles represent the other mRNAs exhibiting a smaller correlation coefficient, and the dark blue circles represent miRNAs. (H) Protein levels of PD-L1 and expression levels of LINC02418 in four NSCLC cell lines. (I) Expression levels of LINC02418 and PD-L1 in H1703 or A549 cells following transfection of LINC02418 vector or LINC02418 smart pool of silencers. ***p<0.001, ****p<0.0001 versus the corresponding controls. DEG, differentially expressed gene; FC, fold change; lncRNA, long non-coding RNA; LUAD, lung adenocarcinoma; LUSC, lung squamous cell carcinoma; mRNA, messenger RNA; NSCLC, non-small cell lung cancer; PD-L1, programmed cell death ligand 1. TCGA, the cancer genome atlas; WGCNA, weighted correlation network analysis.

suggest that there is a negative relation between LIN02418 and PD-L1. In addition, LINC02418 may play a role in the regulation of CD8+T cell infiltration in NSCLC.

LINC02418 dampens PD-1 binding ability and enhances T cell-induced apoptosis in NSCLC

To explore the potential biological functions of LINC02418 in the regulation of PD-L1 expression, we conducted gene set enrichment analysis on RNA-sequencing data of NSCLC from the TCGA database.

Interestingly, the analysis revealed that higher LINC02418 expression was positively correlated with apoptosis and the T-cell receptor signaling pathway (online supplemental figure S2). To verify whether LINC02418 has an inhibitory effect on PD-L1 which locates at cell surface, we transfected A549 cells with scrambled siRNA or LINC02418 smart pool silencers, and transfected H1703 cells with empty vector or LINC02418 expression vector. The transfected cells were incubated with allophycocyanin (APC) anti-human PD-L1 mAb, and the changes in PD-L1 density and content were analyzed by immunofluorescence and flow cytometric (FCM) surface staining. The results showed that knockdown of LINC02418 significantly increased the PD-L1 expression on the surface of A549 cells, while overexpression of LINC02418 decreased the PD-L1 expression on the surface of A549 and H1703 cells (figure 2A,B). As expected, PD-L1 can be triggered by interferon-γ. Similarly, knockdown of LINC02418 also increased the expression of PD-L1 (figure 2B). To test whether LINC02418-mediated regulation of PD-L1 affects the binding of PD-L1 and PD-1, NSCLC cells with LINC02418 overexpression or knockdown were incubated with recombinant human PD-1 Fc protein. FCM assays showed that knockdown of LINC02418 significantly increased the binding of PD-1 to the surface of A549 cells, while LINC02418 overexpression decreased the binding of PD-1 to the surface of H1703 (figure 2C). With the alteration of PD-L1 and PD-1 binding ability, we confirmed the sensitivity of NSCLC cells to T cell-induced apoptosis by co-culturing NSCLC cells with the activated human PBMCs (figure 2D). Hoechst33342/propidium iodide (PI) combined with annexin-V/PI double staining demonstrated that LINC02418 increased the rate of NSCLC cell death co-incubated with activated T cell, indicating that LINC02418 enhances the T cell-induced apoptosis in NSCLC (figure 2E,F). To determine whether the effects observed following T-cell killing are direct or indirect after adding or removing LINC02418, we treated the indicated cells with anti-PD-L1. As anticipated, the addition of anti-PD-L1 significantly reduced the ability of LINC02418 to regulate the rate of A549 cell death and apoptosis co-incubated with activated T cells, indicating that LINC02418 directly modulates T cell-induced apoptosis through PD-L1 (figure 2E,F).

To better reflect tumor specific mechanisms, we illustrated the effect in an antigen-specific model simulating the T-cell receptor (TCR)-major histocompatibility complex (MHC)-peptide interactions between T cells and tumor cells. T cells from the spleens of OT1 mice (#C001198, Cyagen, China) were isolated and co-cultured with mouse LLC tumor cells transfected with OVA. The results demonstrated that LLC cells overexpressing 493Rik were more susceptible to be killed by CD8+T cells (online supplemental figure S5A–C). These findings suggest that LINC02418 dampens PD-1 binding ability and enhances T cell-induced apoptosis in NSCLC.

LINC02418 regulates PD-L1 protein stability through enhancement of the Trim21-mediated ubiquitin-proteasome pathway

Subcellular localization assay demonstrated that LINC02418 was mainly localized in the cytoplasm, which was further verified by RNA fluorescence in situ hybridization (figure 3A,B). We used CHX, a protein synthesis inhibitor, to treat A549 cells. After the addition of CHX, we observed that PD-L1 protein was significantly degraded within approximately 4 hours. However, in A549 cells with LINC02418 knocked down, the degradation of PD-L1 was not significant. This indicates that LINC02418 plays a role in the stability and degradation of PD-L1 (online supplemental figure S3A). Interestingly, addition of the proteasome inhibitor MG132 almost blocked LINC02418 overexpression-mediated PD-L1 degradation in NSCLC cells, suggesting that the ubiquitin-proteasome pathway is involved in LINC02418 modulation of PD-L1 protein stability (figure 3C). Indeed, overexpression of LINC02418 increased PD-L1 ubiquitination (figure 3D).

To identify the E3 ubiquitin ligase responsible for LINC02418 modulation of PD-L1 protein stability, we co-transfected LINC02418 and PD-L1 with some reported E3 ubiquitin ligases of PD-L1 and observed whether LINC02418 affects the binding of PD-L1 and E3 ubiquitin ligases.[17–20] Interestingly, LINC02418 only increased the interaction between Trim21 and PD-L1, which was chosen for further study (online supplemental figure S3B). Ubiquitination assay confirmed that LINC02418 enhances Trim21-mediated PD-L1 ubiquitination (figure 3E). Moreover, RNA immunoprecipitation (RIP) assays demonstrated that LINC02418 was markedly enriched in Trim21 and PD-L1 immunoprecipitates (figure 3F). Deletion mutants of PD-L1-Δ259-290aa and Trim21-Δ16-55aa, as determined by measuring coprecipitated RNA by quantitative real-time polymerase chain reaction (qRT-PCR), failed to interact with LINC02418 (online supplemental figure S4A). On the other hand, co-immunoprecipitation assays showed that LINC02418 (1101–1630 nt) interacted with PD-L1 and LINC02418 (2661–3211 nt) interacted with Trim21 (online supplemental figure S4B). These results indicated that PD-L1 and E3 ubiquitin ligase Trim21 specifically interacted with LINC02418 in NSCLC cells.

Next, we investigated whether LINC02418 changes the colocalization of Trim21 and PD-L1. Overexpression of LINC02418 markedly increased the colocalization of Trim21 and PD-L1 (figure 3G). These data suggest that Trim21 is involved in the regulation of PD-L1 ubiquitination by LINC02418. Consistent with the effects of LINC02418 on Trim21-mediated PD-L1 ubiquitination, LINC02418 increased the interaction between Trim21 and PD-L1 (figure 3H). Knockout of Trim21 by CRISPR/Cas9 technique in A549 cells almost abolished the effect of LINC02418 on PD-L1 degradation (figure 3I,J and online supplemental figure S4C). Taken together, these results suggest that LINC02418 regulates PD-L1 protein

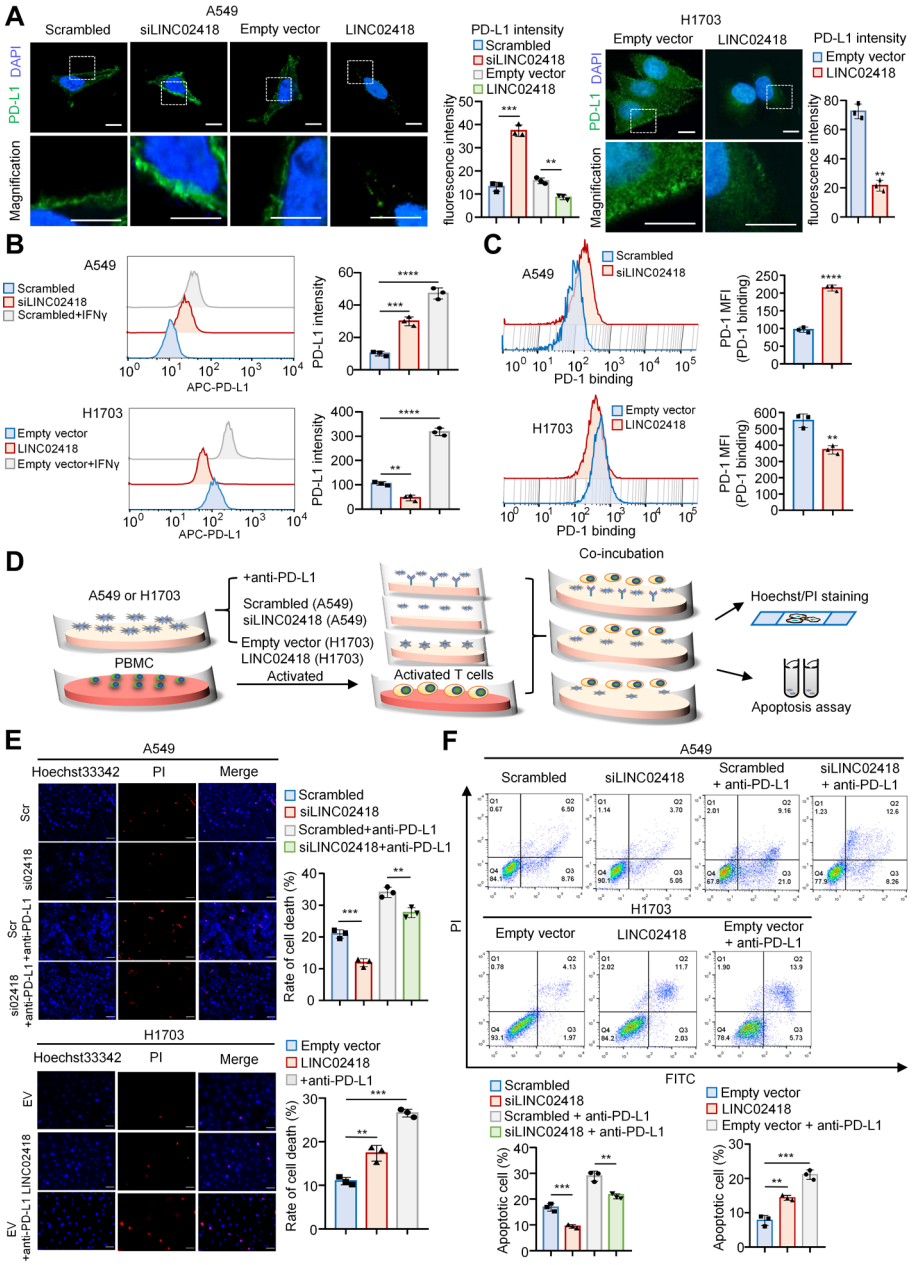

Figure 2 LINC02418 dampens PD-1 binding ability and enhances T cell-dependent toxicity in NSCLC. (A) Immunofluorescence analysis of PD-L1 expression in A549 cells treated with the LINC02418 smart pool of silencers (siLINC02418) or scrambled siRNA (scrambled), as well as in A549 cells or H1703 cells treated with either empty vector or LINC02418. Scale bars represent 10 µm in all panels. (B) FCM was used to detect PD-L1 expression on the surface of NSCLC cells with different conditions. (C) FCM was used to detect the intensity of fluorescence binding to PD-1 of NSCLC cells with different conditions. The PD-1 mean fluorescence intensity (MFI) graph was plotted. (D) Schematic diagram of the effect of LINC02418 on tumor cells killing by PBMC. (E) Hoechst 33342/PI staining assay was used to determine the effect of LINC02418 on PBMC cytotoxicity, with histograms showing the rate of cell death. (F) Cell apoptosis assay was used to determine the effect of LINC02418 on PBMC cytotoxicity, with histograms showing the proportion of apoptotic cells. All experiments were conducted three times, and the results were similar. All values were presented as mean±SD, and statistical differences were calculated using two-sided Student's t-test. **p<0.01, ***p<0.001, ****p<0.0001 versus the corresponding control. APC, allophycocyanin; DAPI, 4',6-Diamidine-2'-phenylindole dihydrochloride; FCM, flow cytometric; FITC, fluorescein Isothiocyanate; IFN, interferon; PBMC, peripheral blood mononuclear cell; PD-1, programmed death 1; PD-L1, programmed cell death ligand 1; PI, propidium iodide; NSCLC, non-small cell lung cancer.

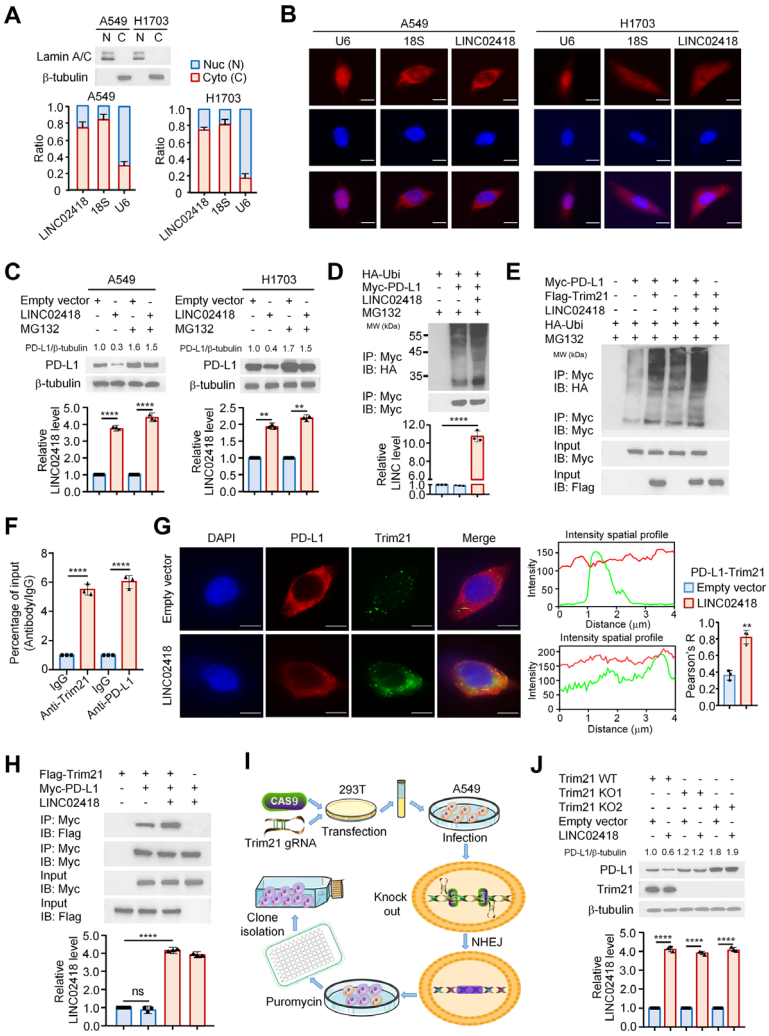

Figure 3 LINC02418 regulates PD-L1 protein stability through enhancing the Trim21-mediated ubiquitin-proteasome pathway. (A) LINC02418 expression in H1703 and A549 cells was detected using qRT-PCR. The separated nucleus and cytoplasm fractions were assessed using western blot assays, with lamin A/C and β-tubulin selected as markers, respectively. (B) Subcellular localization of LINC02418 (red), U6 (nuclear marker, red), and 18S (cytoplasmic marker, red) in H1703 and A549 cells was observed using fluorescence in situ hybridization. The nuclei were stained blue by 4',6-Diamidine-2'-phenylindole dihydrochloride (DAPI). Scale bar, 10 μm. (C) H1703 and A549 cells were transfected with empty vector or LINC02418 and treated with the proteasome inhibitor MG132 (10 μM). PD-L1 expression was detected by Western blot. Histograms showed corresponding expression levels of LINC02418 measured by qRT-PCR. (D) Effects of LINC02418 on the ubiquitination of PD-L1 was analyzed by immunoprecipitation treated with MG132 and incubated with indicated antibodies. (E) Effects of LINC02418 on Trim21-mediated PD-L1 ubiquitination. (F) The interaction between LINC02418 with Trim21 and PD-L1 were assessed by an RNA immunoprecipitation assay. (G) Immunofluorescence showed the co-localization of PD-L1/Trim21 under empty vector and LINC02418 vector transfection in A549 cells. The intensity distribution of PD-L1/Trim21 was plotted in the middle panel, and the statistical quantification of colocalization (Pearson's R value) was shown on the right panel. Values were presented as mean ± SD from three independent experiments, with comparison using a two-sided Student's t-test. Scale bar, 10 μm. (H) Co-immunoprecipitation was performed using lysates of A549 cells expressing Flag-Trim21 and Myc-PD-L1 with or without overexpression of LINC02418. (I) Schematic diagram of the construction of Trim21 knockout (KO) A549 cell lines. (J) Immunoblot analysis of PD-L1 in A549 cells with Trim21 KO cells (Trim21 KO1, Trim21 KO2) stably transfected with empty vector or LINC02418 vector. **p<0.01, ***p<0.001, ****p<0.0001 versus the corresponding control, ns means no significance.IP, immunoprecipitation; IB, immunoblotting; PD-L1, programmed cell death ligand 1; qRT-PCR, quantitative real-time polymerase chain reaction; WT, wildtype.

stability through the enhancement of the Trim21-mediated ubiquitin-proteasome pathway.

LINC02418 downregulates PD-L1 expression and enhances T cell-induced apoptosis dependent on Trim21 in NSCLC

To confirm whether the enhancement of LINC02418 on T cell-induced apoptosis requires the participation of Trim21, we conducted the PD-L1 expression and T cell-induced apoptosis assay in Trim21 knockout A549 cells. Immunofluorescence and western blot assays revealed that LINC02418 overexpression inhibited the expression of PD-L1 in A549 cells, while Trim21 knockout increased PD-L1 expression (figure 4A). Importantly, Trim21 knockout greatly attenuated the ability of LINC02418 to regulate PD-L1 expression, suggesting that LINC02418

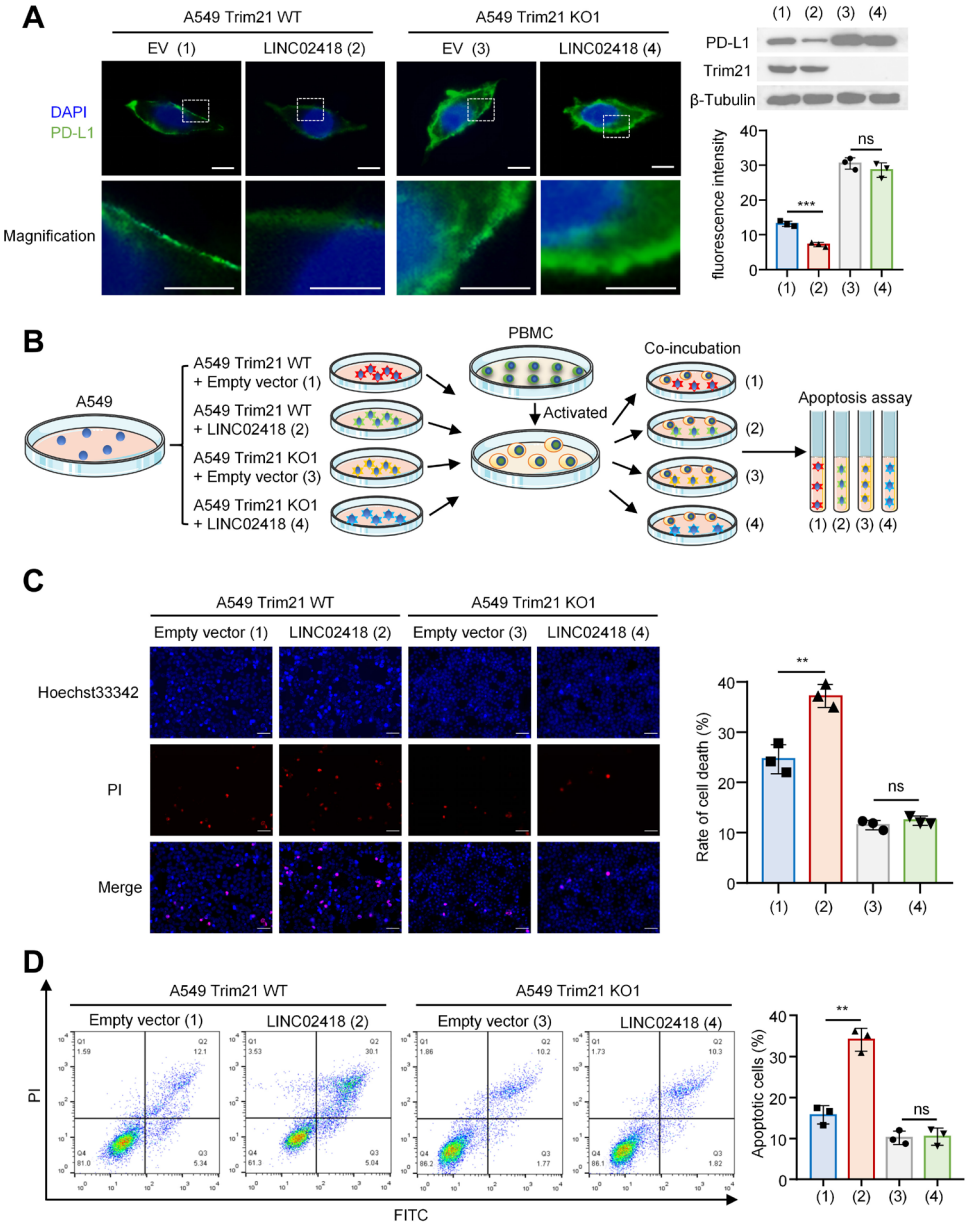

Figure 4 LINC02418 downregulates PD-L1 expression and enhances T cell-induced apoptosis dependent on Trim21 in NSCLC. (A) A549 cells with either Trim21 WT or knockout (Trim21 KO1) were transfected with either empty vector (EV) or LINC02418, and immunofluorescence was used to analyze PD-L1 expression. The histogram displayed the fluorescence intensity on the cell surfaces. (B) Schematic diagram showed the verification of the effect of LINC02418 on T cell-dependent toxicity via Trim21. (C) Hoechst33342/PI staining assay was used to verify whether the effect of LIINC02418 on T cell-induced apoptosis required Trim21 participation. The histogram showed the apoptotic rate of the indicated groups. (D) Apoptosis test was used to verify the effect of LINC02418 on T cell-induced apoptosis in one representative clone of the A549 Trim21 knockout cell lines (Trim21 KO1). The histogram showed the apoptosis rate of the indicated groups. **p<0.01, ***p<0.001 versus the corresponding control, ns means no significance. DAPI, 4',6-Diamidine-2'-phenylindole dihydrochloride; FITC, fluorescein Isothiocyanate; PBMC, peripheral blood mononuclear cell; PD-L1, programmed cell death ligand 1; PI, propidium iodide; WT, wildtype.

regulates PD-L1 expression dependent on Trim21 expression. Next, we investigated whether LINC02418 enhances T cell-induced apoptosis via Trim21. As expected, LINC02418 enhanced T cell-induced apoptosis. However, Trim21 knockout impaired the ability of LINC02418 to enhance T cell-induced apoptosis (figure 4B–D). Taken together, these results suggest that LINC02418 regulates PD-L1 expression and enhances T cell-induced apoptosis in a Trim21-dependent manner in NSCLC.

Mmu-4930573I07Rik, the homologous RNA of hsa-LINC02418 in mouse, enhances the in vivo efficacy of PD-L1 antibody therapy in NSCLC

Based on the fact that LINC02418 enhances T cell-induced apoptosis *in vitro*, we investigated the phenotype of whether LINC02418 enhances the efficacy of PD-L1 antibody therapy in mice. Since the mouse homologous RNA of hsa-LINC02418 is mmu-4930573I07Rik, we obtained stable expression LLC cell lines infected with mmu-4930573I07Rik or an empty vector and subcutaneously injected LLCs into C57BL/6 mice. Once palpable tumors developed (on day 7), we intraperitoneally (ip) injected PD-L1 mAb or IgG2b (as control) every 3 days (5 mg/kg) (figure 5A). Although either PD-L1 mAb treatment or overexpression of mmu-4930573I07Rik could slow down the growth of LLC tumors, no mice survived for more than 35 days after tumor inoculation. Notably, PD-L1 mAb treatment along with overexpression of mmu-4930573I07Rik remarkably inhibited tumor growth, and 2 out of 14 tumor-bearing mice survived for more than 50 days after tumor inoculation (figure 5B,C). As expected, PD-L1 mAb treatment slightly decreased the proportion of Ki-67 positive cells and elevated proportion of apoptotic cells. Moreover, mmu-4930573I07Rik enhanced the efficacy of PD-L1 mAb therapy, with significantly decreased proportion of Ki-67 positive cells and elevated proportion of apoptotic cells compared with mono PD-L1 mAb treatment group (figure 5D). These data suggest that mmu-4930573I07Rik, the mouse homologous RNA of hsa-LINC02418, enhances the efficacy of PD-L1 antibody therapy on NSCLC growth in mice. To further elucidate the dependency of the *in vivo* response to CD8+T cells, we generated a mouse model deficient for CD8+T cells by ip injecting the CD8α antibody (online supplemental figure S5D,E). In those CD8-deficient mice, overexpression of 493Rik failed to enhance the efficacy of PD-L1 antibody therapy on NSCLC growth (online supplemental figure S5F). This observation suggests that the enhanced immune cytotoxicity conferred by 493Rik requires the involvement of CD8+T cells.

Since PD-1/PD-L1 inhibitors are mainly used in patients with advanced NSCLC with local or distant metastasis, we investigated whether mmu-4930573I07Rik could enhance the efficacy of PD-L1 mAb to harness the metastatic phenotype of NSCLC *in vivo* (figure 5E). Consistent with the findings in growth phenotype, mmu-4930573I07Rik enhanced the in vivo efficacy of PD-L1 antibody therapy in controlling the metastatic phenotype of NSCLC (figure 5F,G).

Hsa-LINC02418 and mmu-4930573I07Rik are m6A-modificated by METTL3 and degraded in a manner dependent on the m6A reader protein YTHDF2

To explore how hsa-LINC02418 and mmu-4930573I07Rik were regulated, we focused on m6A RNA methylation, a predominant RNA modification that occurs in eukaryotic cells. To verify our hypothesis, STM2457, the inhibitor of m6A methyltransferase METTL3, and FB23, the inhibitor of demethylase fat mass and obesity-associated protein (FTO), were added to verify if the methylase and demethylase were responsible for regulation of hsa-LINC02418 and mmu-4930573I07Rik expression. Results showed that METTL3 rather than FTO was responsible for the regulation of hsa-LINC02418 and mmu-4930573I07Rik expression, as evident from the marked increase in their levels following STM2457 addition, while FB23 had no effect (figure 6A and online supplemental figure S6A). Prediction of the m6A-modification site revealed that two out of nine m6A sites in hsa-LINC02418 and one m6A site in mmu-4930573I07Rik sequences had adequate confidence (http://www.cuilab.cn/sramp) (figure 6B,C and online supplemental figure S6B,C). RIP assay was conducted to confirm the RNA and METTL3 binding, which showed that METTL3 could bind to the predicted m6A sites of hsa-LINC02418 and mmu-4930573I07Rik, respectively (figure 6D and online supplemental figure S6D). Next, the wildtype (WT) and mutant luciferase reporter vectors of the predicted m6A sites in A549 and H1703 cells as well as in LLC cells were co-transfected with or without hsa-METTL3 or mmu-mettl3 plasmid. The luciferase reporter assay demonstrated that METTL3 significantly suppressed the luciferase activity of WT plasmid with m6A binding sites but not that of plasmid with mutated m6A binding site (figure 6E and online supplemental figure S6E). To further detect the stability of hsa-LINC02418 and mmu-4930573I07Rik, STM2457 was added into NSCLC or LLC cells followed by the treatment of actinomycin D. The results demonstrated that STM2457 prolongs the stability of hsa-LINC02418 and mmu-4930573I07Rik, indicating that METTL3 impairs the stability of hsa-LINC02418 and mmu-4930573I07Rik (figure 6F,G and online supplemental figure S6F).

During the process from DNA to RNA, adenylate is methylated at the sixth N position by methylation enzymes, such as METTL3. Then, some enzymes recognize the base of m6A methylation and participate in downstream translation and mRNA degradation. It is known that the YTHDF family, especially the YTHDF2 enzyme, participates in the mRNA degradation process. Therefore, we tested if YTHDF2 affects the RNA stability of hsa-LINC02418 and mmu-4930573I07Rik. RIP assay demonstrated that YTHDF2 bound to the predicted m6A sites of hsa-LINC02418 and mmu-4930573I07Rik (figure 6H and online supplemental figure S6G). Importantly, knockdown of YTHDF2 significantly increased

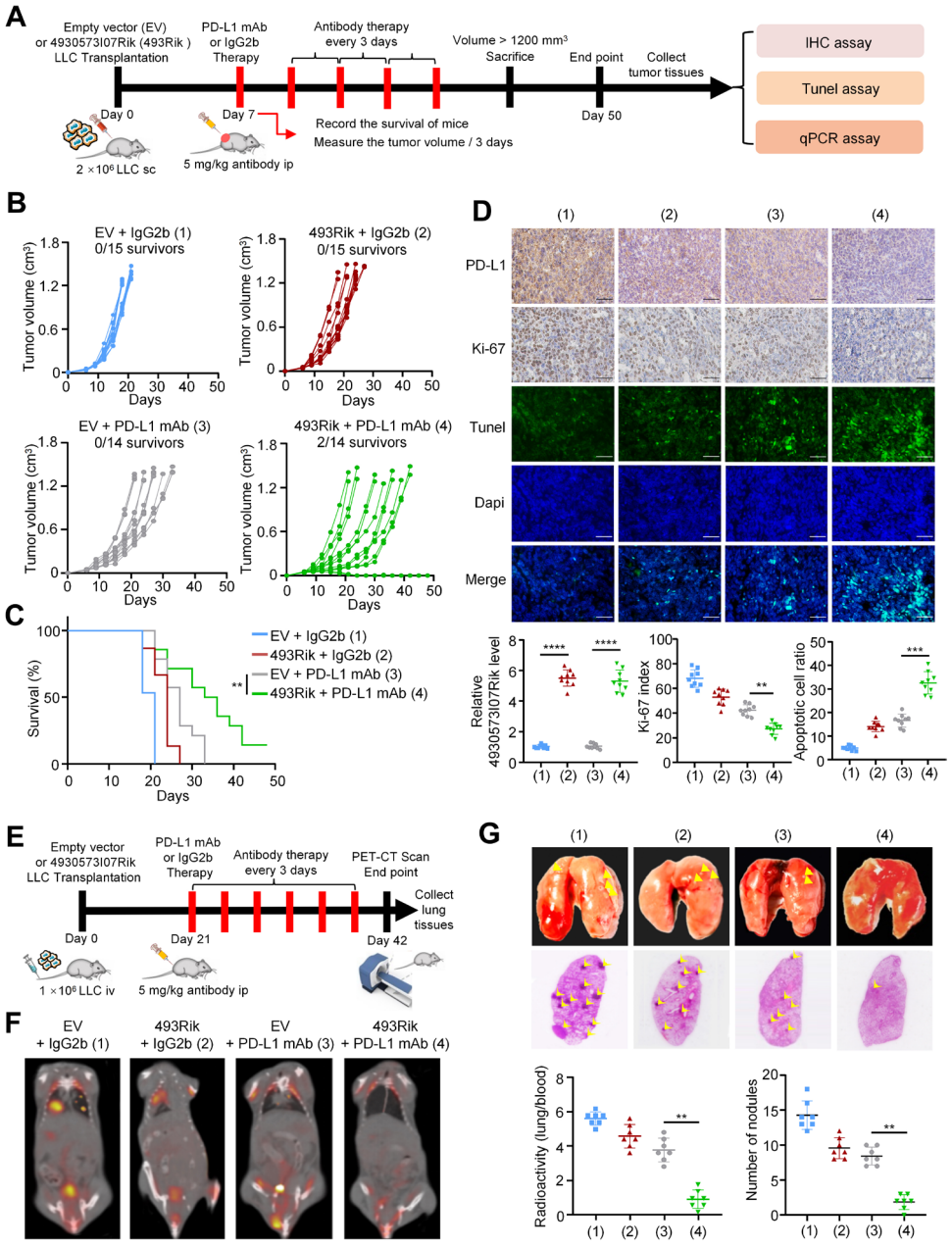

Figure 5 Mmu-4930573I07Rik (493Rik), the mouse homologous RNA of hsa-LINC02418, enhances the efficacy of PD-L1 antibody therapy in vivo. (A) The experimental scheme of the in vivo study. (B) Volumes of LLC tumors carrying empty vector (treated with IgG2b, blue lines, n=15; treated with anti-PD-L1 mAb, gray lines, n=14), or 493Rik vector (treated with IgG2b, red lines, n=15; treated with anti-PD-L1 mAb, green lines, n=14) were plotted individually. (C) Kaplan-Meier survival curves for each group. The p value was calculated using a two-sided Gehan-Breslow-Wilcoxon test. (D) The top two rows were representative IHC staining of PD-L1 and Ki67 of the collected tumors. The histograms showed the 493Rik levels determined by qRT-PCR and Ki-67 index determined by proportion of positive cell count. The lower three rows were representative Tunel staining of the collected tumors. The histogram showed the apoptotic cell ratio. Scale bar, 50 µm. (E) The experimental scheme of the in vivo study of lung metastasis. (F) The representative PET-CT scan images of the mice in each group. (G) Representative lung tissue anatomy and H&E staining pictures of the mice. The histogram showed the number of tumor nodules observed under the microscope. *p<0.05, **p<0.01, ***p<0.001, ****p<0.0001 versus the corresponding control, ns means no significance. IHC, immunohistochemistry; LLC, Lewis lung carcinoma cell; mAb, monoclonal Antibody; PD-L1, programmed cell death ligand 1; PET-CT, positron emission tomography-CT; qRT-PCR, quantitative real-time polymerase chain reaction.

the mRNA levels and prolonged the stability of hsa-LINC02418 and mmu-4930573I07Rik, indicating that YTHDF2 is responsible for the degradation of hsa-LINC02418 and mmu-4930573I07Rik (figure 6I–K and online supplemental figure S6H). Taken together, these data suggest hsa-LINC02418 and mmu-4930573I07Rik are m6A-modificated by METTL3 and degraded in a manner dependent on the m6A reader protein YTHDF2. As expected, treatment of STM2457 markedly decreased the level of PD-L1 expression and increased that of PD-L1

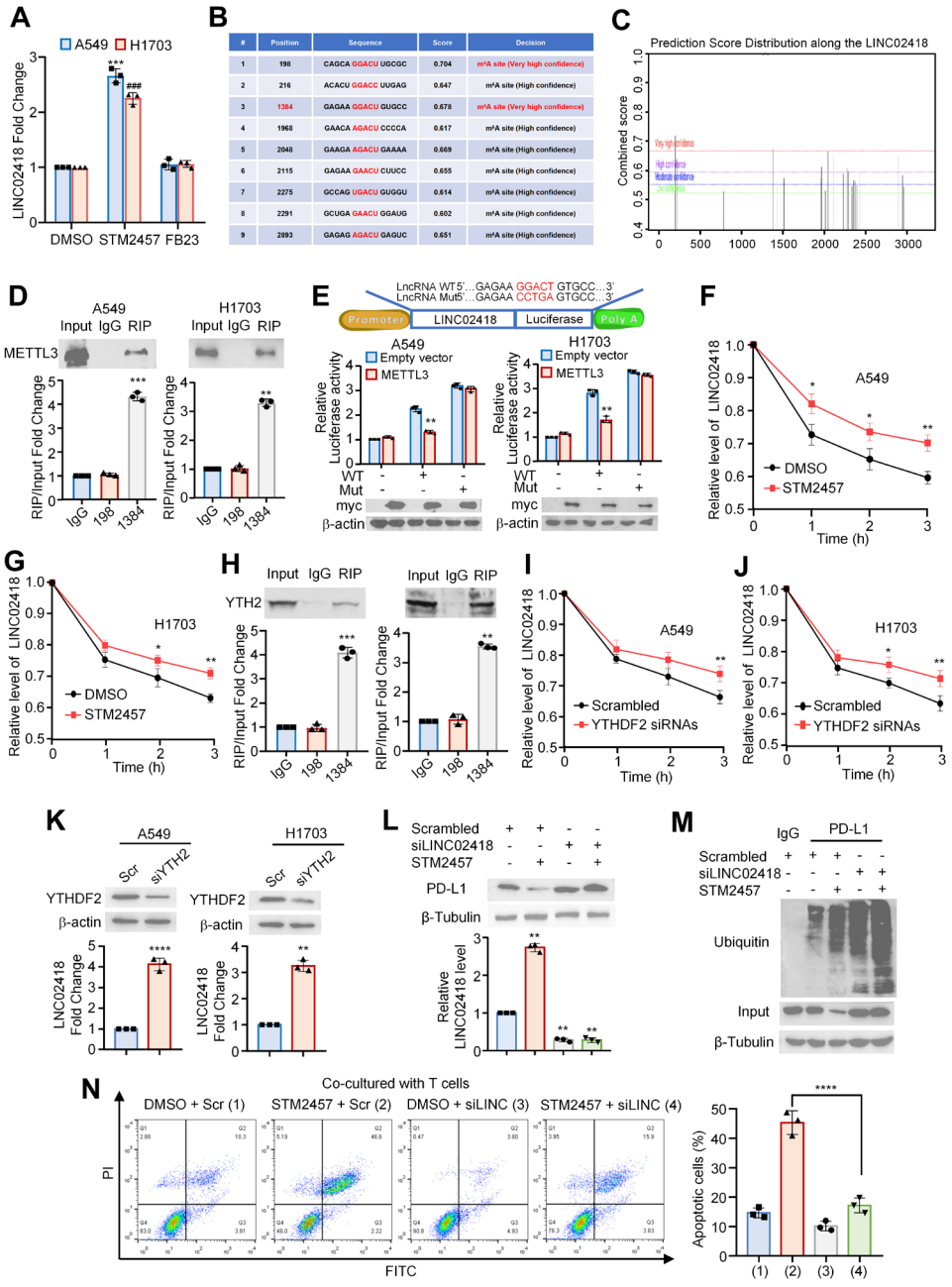

Figure 6 Hsa-LINC02418 is m6A-modificated by METTL3 and degraded in a manner dependent on the m6A reader protein YTHDF2. (A) The expression level of LINC02418 in A549 and H1703 cells treated with DMSO, STM2457 or FB23, respectively. (B) The prediction score distribution along the LINC02418 sequence. (C) The specific possible position of m6A sites in the LINC02418 sequence. (D) RIP-RT-PCR assays for detection of the two m6A sites in A549 and H1703 cell lysates immunoprecipitated with METTL3 antibody. (E) The upper panel showed the sequence scheme of the wild-type (WT) and mutant (Mut) luciferase reporter plasmids. The lower panel showed the luciferase activity after co-transfection of LINC02418 WT or LINC02418 Mut plasmid with myc tagged METTL3 plasmid or empty vector. (F) The mRNA levels of LINC02418 were detected at different time points after treated with STM2457 or DMSO in A549 cells. (G) The mRNA levels of LINC02418 were detected at different time points after treated with STM2457 or DMSO in H1703 cells. (H) Two m6A sites with very high confidence were detected by qRT-PCR assay after immunoprecipitated with YTHDF2 antibody. The mRNA level of LINC02418 were detected at different time points after treated with YTHDF2 siRNAs or scrambled in (I) A549 cells and (J) H1703 cells, respectively. (K) The fold change of LINC02418 in A549 and H1703 cells under YTHDF2 gene was knocked down with specific siRNAs. (L) The mRNA level and protein expression level of PD-L1 in A549 cells which were treated by LINC02418 siRNAs or scrambled siRNAs with or without STM2457. (M) Immunoprecipitation and immunoblotting analysis of A549 cells treated by LINC02418 siRNAs or scrambled siRNAs with or without STM2457. (N) Apoptosis assay tested T-cell cytotoxic effect to A549 cells treated by LINC02418 siRNAs or scrambled siRNAs with or without STM2457. The histogram showed the percentage of apoptosis cells. Data are presented as mean±SD, $^{*}p<0.05$, $^{**}p<0.01$, $^{***}p<0.001$, $^{****}p<0.0001$ versus the corresponding control. DMSO, Dimethyl sulfoxidem; FITC, fluorescein Isothiocyanate; mRNA, messenger RNA; PD-L1, programmed cell death ligand 1; RIP, RNA immunoprecipitation; qRT-PCR, quantitative real-time polymerase chain reaction.

ubiquitination as well as T cell-induced apoptosis, and more importantly, these effects could be attenuated when LINC02418 was silenced, indicating that METTL3 regulates PD-L1 expression, PD-L1 ubiquitination and T cell-induced apoptosis (figure 6L–N).

Correlations of the expression of LINC02418, PD-L1 and T immune cell infiltration in human NSCLC

The expression of LINC02418 was evaluated in 54 human NSCLC samples by fluorescence in situ hybridization staining and the expression of PD-L1 was evaluated by IHC staining (online supplemental figure S7). Consistent with cultured cell assays, the expression of LINC02418 in NSCLC was negatively correlated with the expression of PD-L1 and positively correlated with the infiltration of CD8+T cells, with no obvious correlation with CD4+T cells (figure 7A). In order to understand the fine-tune modulation of immune infiltration by LINC02418, 521 NSCLC samples were divided into LIN02418 high and low expression group and analyzed for the difference in both groups for the proportion of immune cell infiltration using the CIBESORT algorithm. For the whole NSCLC cohort, the proportion of T immune cell infiltration demonstrated little difference between the two groups (online supplemental figure S8A,B). However, when the whole NSCLC cohort was subdivided into Trim21 positive and negative group, it was interesting to observe that CD8+T cells were markedly increased in the Trim21 positive group with high expression of LIN02418, which demonstrated no difference in the Trim21 negative group (figure 7B,C). These data collectively indicates that in NSCLC tissue, LINC02418 enhanced CD8+T cell immune response dependent on Trim21 status.

DISCUSSION

Immunotherapy has become a research hotspot for cancer treatment. The PD-1/PD-L1 immune blockade therapy is the most typical representative of immunotherapy. As a ligand of the immunosuppressive molecule PD-1, PD-L1 can inhibit the killing ability of T cells to a large extent, thereby promoting tumor progression.[21] Recent studies have found that PD-L1 is not only expressed on tumor cells (tPD-L1), but also on myeloid cells like dendritic cells and macrophages (mPD-L1).[22] The expression of mPD-L1 is considered as an important factor in inhibiting T cell-mediated antitumor response and promoting immune evasion.[23] However, when some research findings of mPD-L1 in mouse models were applied to patients with cancer who had undergone immune therapy, the results were not always consistent.[24] While some clinical trials have shown that tPD-L1 expression is still the strongest predictor of patient survival, others suggest that combining PD-L1 expression on both tumor cells and immune cells could be a better indicator.[25 26] Nevertheless, the significance of tPD-L1 expression in immunotherapy should still be valued. PD-L1 is overexpressed in multiple tumor cells including NSCLC and high PD-L1 level predicts poorer relapse-free and OS in patients with NSCLC.[27 28] In addition, overexpression of PD-L1 promotes cancer cell to escape from immune surveillance in NSCLC.[29 30] There have been several studies on the positive regulators of PD-L1 expression in NSCLC.[31–33] However, the upstream negative factors of PD-L1 and how they regulate PD-L1 expression remain largely unknown. As to lncRNAs, the negative regulating lncRNAs of PD-L1 expression have not been reported yet. In our current study, we identified a novel negatively-regulating lncRNA, LINC02418, to decrease PD-L1 expression and enhance PD-L1 immune therapy response via Trim21. LINC02418 and Trim21 are novel upstream negative regulators of PD-L1. In NSCLC cells, LINC02418 inhibits PD-1 binding ability and enhances T cell-induced apoptosis dependent on Trim21 both in vitro and in vivo. Mechanistically, LINC02418 regulates PD-L1 protein stability through enhancing the Trim21-mediated ubiquitin-proteasome pathway. Moreover, in NSCLC samples, the expression of LINC02418 in NSCLC was negatively correlated with the expression of PD-L1 and positively correlated with the infiltration of CD8+T cells. Thus, our data establishes the physiological and pathological significance of LINC02418 or Trim21 in regulating PD-L1-mediated immune checkpoint therapeutic response. Supplement of LINC02418 or Trim21 may be beneficial to enhancing the response to PD-1/PD-L1 blockade therapy.

It has been found that PD-L1 protein has various post-translational modifications (PTM) which play key roles in regulating PD-L1 stability and expression level.[34] Developing strategies to target the PTM of PD-L1 protein, with the aim of eliminating PD-L1 from both the surface and interior of tumor cells, will hold great potential for enhancing the effectiveness of immunotherapeutic approaches focused on PD-L1. Ubiquitination is an important PTM that reduces PD-L1 expression. β-TrCP is an E3 ligase responsible for polyubiquitination and destabilization of aglycosylated PD-L1 and degrades PD-L1 protein in triple-negative breast cancer cells.[19] Mezzadra *et al* verified that STUB1 is an E3 ligase that degrades PD-L1, and CMTM6 protects the stability of PD-L1 by inhibiting STUB1 and preventing ubiquitination.[18] Gao *et al* found that knockdown of the cyclin-dependent kinase CDK5 in lung adenocarcinoma promoted the E3 ligase Trim21 to degrade PD-L1 by ubiquitination.[20] Wu *et al* demonstrated that the E3 ligase ARIH1 mediates PD-L1 ubiquitination and degradation in tumors.[17] In our study, we found that the degradation of PD-L1 by LINC02418 was mainly mediated by the E3 ligase Trim21. Overexpression of LINC02418 enhanced the binding of Trim21 to PD-L1 and the killing of NSCLC cells by activated PBMC cells.

In the past, it was believed that a prerequisite for the application of PD-L1 monoclonal antibody was the expression of PD-L1, which had to be greater than 50%.[35] However, a recent study showed that PD-L1 expression is not an absolutely accurate prerequisite factor for the application of the PD-L1 monoclonal antibody. Even if some patients with NSCLC have lower PD-L1 expression,

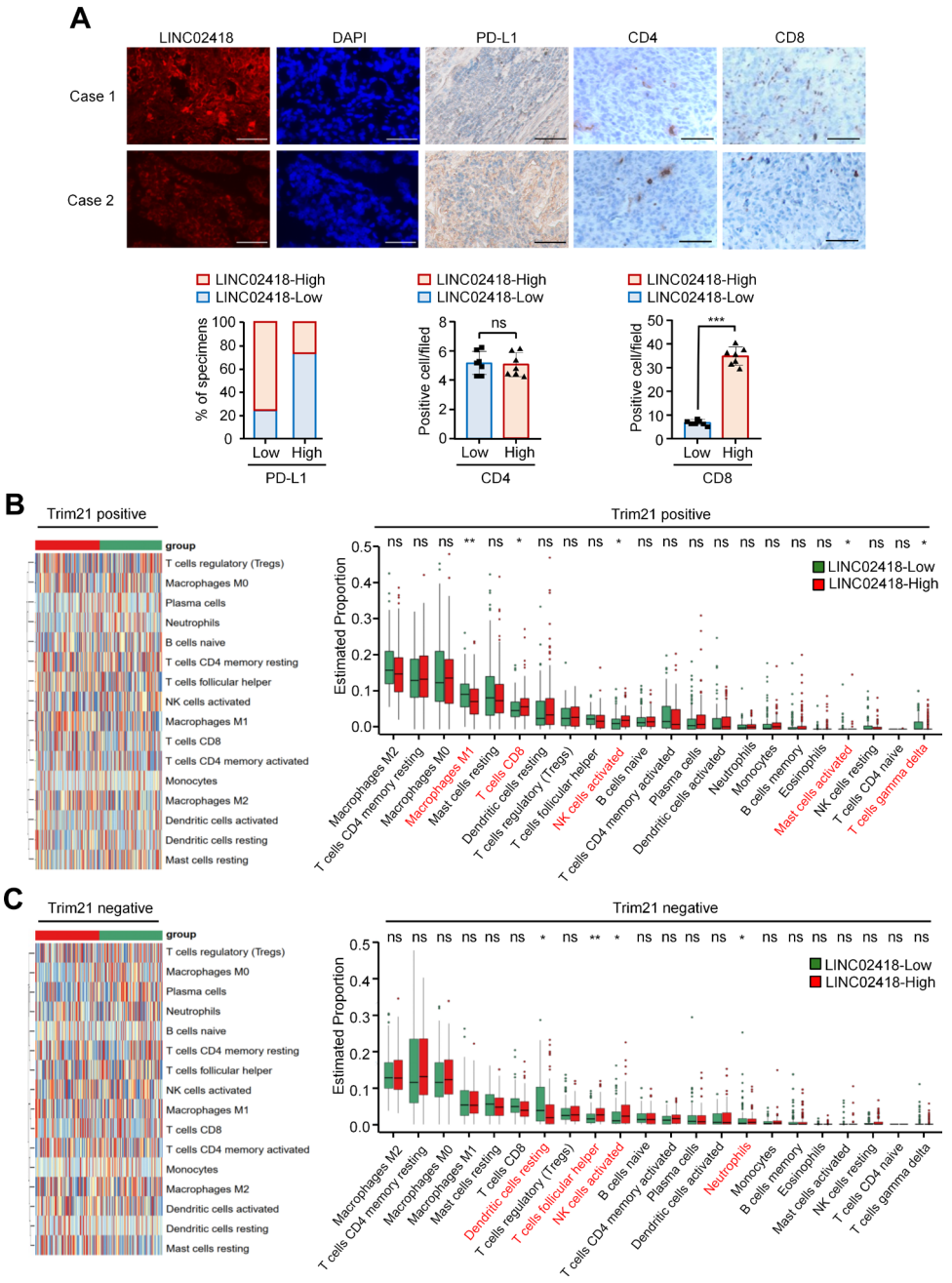

Figure 7 Correlation between the expression of LINC02418, PD-L1 and T immune cell infiltration in human NSCLC. (A) The representative fluorescence in situ hybridization staining of LINC02418 and IHC staining of PD-L1, CD4 and CD8 in tumor sections of clinical NSCLC cases. Scale bar, 50 µm. The lower three histograms showed the percentage of sections with low or high PD-L1 displaying low or high LINC02418 levels in NSCLC specimens, the positive CD4 cell counts and the positive CD8 cell counts. (B, C) In the TCGA database, patients with NSCLC were divided into Trim21 positive and Trim21 negative group. The proportions of immune cells were compared under LINC02418 low or high expression status. *p<0.05, **p<0.01 versus the corresponding control, ns means no significance. DAPI, 4',6-Diamidine-2'-phenylindole dihydrochloride; IHC, immunohistochemistry; NK, natural killer; NSCLC, non-small cell lung cancer; PD-L1, programmed cell death ligand 1; TCGA, the cancer genome atlas.

the therapeutic effects of PD-L1 monoclonal antibody will be obvious.[36] LINC02418 can reduce the expression of PD-L1 in tumor cells, thereby affecting the efficacy of the PD-L1 monoclonal antibody. In our study, we found that the combination of LINC02418 and low-dose PD-L1 mAb yielded favorable effects relative to PD-L1 mAb alone. In vitro and in vivo experiments showed that LINC02418 and mmu-4930573I07Rik exerted synergistic effects with PD-L1 mAb to promote the killing of T cells in tumors, thereby providing certain applicability for clinical tumor treatment.

METTL3 is an m6A RNA methyltransferase that is highly expressed in most cancers, participates in tumor proliferation, differentiation, and metastasis and associates

with poor prognosis of various malignant tumors. The high expression of METTL3 was reported to be associated with the prognosis of various cancers, such as oral squamous cell carcinoma, neck squamous cell carcinoma, hepatocellular carcinoma cells and pancreatic cancer.[37–40] Moreover, a highly potent METTL3 inhibitor, STM2457, exhibited effective therapeutic effect against acute myeloid leukemia.[38] Besides, accompanied with the arising of immunotherapy, the influence of METTL3 on tumor immunity started to draw researchers' attention. It has been reported in various cancers, the high expression of METTL3 facilitated the expression of immunosuppressive immune checkpoint molecule, PD-L1, and negatively correlated with the infiltration of tumor immune cells and inhibited their activities.[39–41] Consequently, METTL3 inhibitor, STM2457, promoted the anti-PD-1 immunotherapy of cervical squamous cell carcinoma in a mouse model.[40] These studies confirmed the immunomodulatory role of METTL3, but with detailed mechanism still unresolved. In our research, LINC02418 was identified as a negative regulator of PD-L1, and thus, the relationship between METTL3 and LINC02418 brought our interests. METTL3 was proven to trigger the degradation of hsa-LINC02418 and mmu-4930573I07Rik via YTHDF2. This gave us a more specific illustration that LINC02418 is one of the downstream effector molecules of METTL3 to execute the regulation of PD-L1.

LINC02418 has been reported in colorectal cancer (CRC). Tian *et al* reported that LINC02418 physically combines with miR-34b-5p and then affects the BCL2 signal pathway, resulting in the growth of CRC cells.[42] Zhao *et al* determined that LINC02418 is significantly overexpressed in CRC and discovered the key role of the LINC02418-miR-1273g-3p-MELK axis in tumorigenesis, thereby providing a new method for clinical diagnosis of CRC.[43] LINC02418 has been reported to promote tumor cell proliferation and survival in NSCLC,[44] while our study revealed a specific role of LINC02418 in immune evasion and its potential therapeutic effect in PD-1/PD-L1 blockade treatment for NSCLC. Our study found that overexpression of LINC02418 in tumor cells enhances T cell-induced cell death and apoptosis. The discrepancy between our study and Han's paper may lie in different focus and study model. Our study mainly investigated the function of LINC02418 in the context of the immune microenvironment, specifically the interaction between tumor cells and immune cells. Therefore, our study model involved co-culturing tumor cells and immune cells, which affected apoptosis and other functions. In contrast, Han's study mainly focused on tumor cells alone and their observed apoptosis. Our study showed that LINC02418 promoted and enhanced the killing effects of immune cells by reducing the PD-L1 expression on tumor cells, thereby indirectly inhibiting the growth of tumors, which may underlie implications for immunotherapy in lung cancer. We not only experimentally validated the function of LINC02418, but also analyzed its relationship to immune infiltration from the TCGA database. In Trim21-positive cases, we found that patients with high expression of LINC02418 expressed more CD8+T cells than patients with low expression of LINC02418, which is consistent with our experimental conclusions.

In conclusion, LINC02418 is a novel negative regulator of PD-L1 and plays a crucial role in immune evasion in NSCLC. This study sheds light on the novel mechanisms of PD-L1 negative regulation and provides a rationale for enhancing the effectiveness of anti-PD-L1 treatment in NSCLC.

Author affiliations
[1]Department of Genetic Engineering, Beijing Institute of Biotechnology, Beijing, China
[2]Department of Radiation Oncology, Air Force Medical Center PLA, Air Force Medical University, Beijing, China
[3]Department of Urology, the Third Medical Center of PLA General Hospital, Beijing, China
[4]Department of Biotherapy Center, Third People's Hospital, Second Hospital Affiliated to Southern University of Science and Technology, Shenzhen, Guangdong, China
[5]Bioinformatics Center of Academy of Military Medical Sciences, Beijing, China
[6]Department of Oncology, Chinese PLA General Hospital Fifth Medical Center, Beijing, China
[7]Department of Oncology, Chinese PLA General Hospital Second Medical Center, Beijing, China

Contributors ZS, HM, CX, ZF, and JL contributed equally to this work. XX conceived the project, designed the experiments, and analyzed the data. ZS designed and performed the experiments and analyzed the data. HM, CX, ZF, and JL performed the experiments and analyzed the data. NH performed CT scan analysis. HC, XK, CT, LF, HZ, and YH made expression vectors and performed animal experiments. CS and HP collected and analyzed the clinical samples. XX and ZS wrote the manuscript. XX, ND, JY, and YD supervised the study. XX was the guarantor of the study. All authors read and approved the final manuscript.

Funding This work was supported by grants from the National Natural Science Foundation of China (82272762, 82202852, 81972446, 81872090, 82173259, 81972734), Beijing Natural Science Foundation (L222072, 7222232), Beijing Novo Program (20220484176).

Competing interests None declared.

Patient consent for publication Consent obtained directly from patient(s).

Ethics approval Human tissue samples were collected according to the Helsinki Declaration and the study was approved by the Ethics Committee of Beijing Institute of Biotechnology (Approval number AF/SC-08/02.198). Participants gave informed consent to participate in the study before taking part.

Provenance and peer review Not commissioned; externally peer reviewed.

Data availability statement Data are available upon reasonable request. All data relevant to the study are included in the article or uploaded as supplementary information.

ORCID iD
Xiaojie Xu http://orcid.org/0000-0002-7337-4308

REFERENCES

1 Bade BC, Dela Cruz CS. Lung cancer 2020: epidemiology, etiology, and prevention. *Clin Chest Med* 2020;41:1–24.
2 Pardoll DM. The blockade of immune checkpoints in cancer immunotherapy. *Nat Rev Cancer* 2012;12:252–64.
3 Chen Y, Pei Y, Luo J, *et al*. Looking for the optimal PD-1/PD-L1 inhibitor in cancer treatment: a comparison in basic structure, function, and clinical practice. *Front Immunol* 2020;11:1088.
4 Huang M-Y, Jiang X-M, Wang B-L, *et al*. Combination therapy with PD-1/PD-L1 blockade in non-small cell lung cancer: strategies and mechanisms. *Pharmacol Ther* 2021;219:107694.
5 Yang Y, Yu Y, Lu S. Effectiveness of PD-1/PD-L1 inhibitors in the treatment of lung cancer: brightness and challenge. *Sci China Life Sci* 2020;63:1499–514.
6 Shergold AL, Millar R, Nibbs RJB. Understanding and overcoming the resistance of cancer to PD-1/PD-L1 blockade. *Pharmacol Res* 2019;145:104258.
7 Wen M, Cao Y, Wu B, *et al*. PD-L1 degradation is regulated by electrostatic membrane association of its cytoplasmic domain. *Nat Commun* 2021;12:5106.
8 Wu Y, Chen W, Xu ZP, *et al*. PD-L1 distribution and perspective for cancer immunotherapy-blockade, knockdown, or inhibition. *Front Immunol* 2019;10:2022.
9 St. Laurent G, Wahlestedt C, Kapranov P. The landscape of long noncoding RNA classification. *Trends in Genetics* 2015;31:239–51.
10 Mercer TR, Mattick JS. Structure and function of long noncoding RNAs in epigenetic regulation. *Nat Struct Mol Biol* 2013;20:300–7.
11 Herman AB, Tsitsipatis D, Gorospe M. Integrated LncRNA function upon genomic and epigenomic regulation. *Mol Cell* 2022;82:2252–66.
12 Wei S, Wang K, Huang X, *et al*. LncRNA MALAT1 contributes to non-small cell lung cancer progression via modulating miR-200A-3P/programmed death-ligand 1 axis. *Int J Immunopathol Pharmacol* 2019;33:2058738419859699.
13 Chen Z, Chen Z, Xu S, *et al*. LncRNA SOX2-OT/miR-30D-5P/PDK1 regulates PD-L1 checkpoint through the mTOR signaling pathway to promote non-small cell lung cancer progression and immune escape. *Front Genet* 2021;12:674856.
14 Huang W, Chen TQ, Fang K, *et al*. N6-Methyladenosine methyltransferases: functions, regulation, and clinical potential. *J Hematol Oncol* 2021;14:117.
15 Wei L, Wang H, Yang F, *et al*. Interleukin-17 potently increases non-small cell lung cancer growth. *Mol Med Rep* 2016;13:1673–80.
16 Newman AM, Liu CL, Green MR, *et al*. Robust enumeration of cell subsets from tissue expression profiles. *Nat Methods* 2015;12:453–7.
17 Wu Y, Zhang C, Liu X, *et al*. Arih1 signaling promotes anti-tumor immunity by targeting PD-L1 for proteasomal degradation. *Nat Commun* 2021;12:2346.
18 Mezzadra R, Sun C, Jae LT, *et al*. Identification of CMTM6 and CMTM4 as PD-L1 protein regulators. *Nature* 2017;549:106–10.
19 Deng L, Qian G, Zhang S, *et al*. Inhibition of mTOR complex 1/P70 S6 kinase signaling elevates PD-L1 levels in human cancer cells through enhancing protein stabilization accompanied with enhanced beta-Trcp degradation. *Oncogene* 2019;38:6270–82.
20 Gao L, Xia L, Ji W, *et al*. Knockdown of Cdk5 down-regulates PD-L1 via the ubiquitination-proteasome pathway and improves antitumor immunity in lung adenocarcinoma. *Transl Oncol* 2021;14:101148.
21 Sun C, Mezzadra R, Schumacher TN. Regulation and function of the PD-L1 checkpoint. *Immunity* 2018;48:434–52.
22 Oh SA, Wu D-C, Cheung J, *et al*. PD-L1 expression by dendritic cells is a key regulator of T-cell immunity in cancer. *Nat Cancer* 2020;1:681–91.
23 Dammeijer F, van Gulijk M, Mulder EE, *et al*. The PD-1/PD-L1-checkpoint restrains T cell immunity in tumor-draining lymph nodes. *Cancer Cell* 2020;38:685–700.
24 Yoon HH, Jin Z, Kour O, *et al*. Association of PD-L1 expression and other variables with benefit from immune checkpoint inhibition in advanced gastroesophageal cancer: systematic review and meta-analysis of 17 phase 3 randomized clinical trials. *JAMA Oncol* 2022;8:1456–65.
25 Cimino-Mathews A, Thompson E, Taube JM, *et al*. PD-L1 (B7-H1) expression and the immune tumor microenvironment in primary and metastatic breast Carcinomas. *Hum Pathol* 2016;47:52–63.
26 Klement JD, Redd PS, Lu C, *et al*. Tumor PD-L1 engages myeloid PD-1 to suppress type I interferon to impair cytotoxic T lymphocyte recruitment. *Cancer Cell* 2023;41:620–36.
27 Wu P, Wu D, Li L, *et al*. PD-L1 and survival in solid tumors: a meta-analysis. *PLoS ONE* 2015;10:e0131403.
28 Mu CY, Huang JA, Chen Y, *et al*. High expression of PD-L1 in lung cancer may contribute to poor prognosis and tumor cells immune escape through suppressing tumor infiltrating dendritic cells maturation. *Med Oncol* 2011;28:682–8.
29 Lastwika KJ, Wilson W III, Li QK, *et al*. Control of PD-L1 expression by oncogenic activation of the AKT-mTOR pathway in non-small cell lung cancer. *Cancer Res* 2016;76:227–38.
30 Peng S, Wang R, Zhang X, *et al*. EGFR-TKI resistance promotes immune escape in lung cancer via increased PD-L1 expression. *Mol Cancer* 2019;18:165.
31 Kong T, Ahn R, Yang K, *et al*. Cd44 promotes PD-L1 expression and its tumor-intrinsic function in breast and lung cancers. *Cancer Res* 2020;80:444–57.
32 Wang K, Wang J, Liu T, *et al*. Morphine-3-glucuronide upregulates PD-L1 expression via Tlr4 and promotes the immune escape of non-small cell lung cancer. *Cancer Biol Med* 2021;18:155–71.
33 Li Y, Liu H, Zhao Y, *et al*. Tumor-associated macrophages (Tams)-derived osteopontin (OPN) upregulates PD-L1 expression and predicts poor prognosis in non-small cell lung cancer (NSCLC). *Thorac Cancer* 2021;12:2698–709.
34 Hsu JM, Li CW, Lai YJ, *et al*. Posttranslational modifications of PD-L1 and their applications in cancer therapy. *Cancer Res* 2018;78:6349–53.
35 Reck M, Rodríguez-Abreu D, Robinson AG, *et al*. Pembrolizumab versus chemotherapy for PD-L1-positive non-small-cell lung cancer. *N Engl J Med* 2016;375:1823–33.
36 Shen X, Zhao B. Efficacy of PD-1 or PD-L1 inhibitors and PD-L1 expression status in cancer: meta-analysis. *BMJ* 2018;362:k3529.
37 Ai Y, Liu S, Luo H, *et al*. METTL3 Intensifies the progress of oral squamous cell carcinoma via modulating the M6A amount of Prmt5 and PD-L1. *J Immunol Res* 2021;2021:6149558.
38 Pan F, Lin XR, Hao LP, *et al*. The role of RNA methyltransferase METTL3 in hepatocellular carcinoma: results and perspectives. *Front Cell Dev Biol* 2021;9:674919.
39 Song Z, Wang X, Chen F, *et al*. LncRNA MALAT1 regulates METTL3-mediated PD-L1 expression and immune infiltrates in Pancreatic cancer. *Front Oncol* 2022;12:12.
40 Yu R, Wei Y, He C, *et al*. Integrative analyses of M6A regulators identify that METTL3 is associated with HPV status and immunosuppressive Microenvironment in HPV-related cancers. *Int J Biol Sci* 2022;18:3874–87.
41 Wan W, Ao X, Chen Q, *et al*. METTL3/IGF2BP3 axis inhibits tumor immune surveillance by upregulating N(6)-methyladenosine modification of PD-L1 mRNA in breast cancer. *Mol Cancer* 2022;21:60.
42 Tian J, Cui P, Li Y, *et al*. LINC02418 promotes colon cancer progression by suppressing apoptosis via interaction with miR-34B-5P/Bcl2 axis. *Cancer Cell Int* 2020;20:460.
43 Zhao Y, Du T, Du L, *et al*. Long noncoding RNA LINC02418 regulates MELK expression by acting as a ceRNA and may serve as a diagnostic marker for colorectal cancer. *Cell Death Dis* 2019;10:568.
44 Han B. LncRNA LINC02418 regulates proliferation and apoptosis of non-small cell lung cancer cells by regulating miR-4677-3p/SEC61G. *Eur Rev Med Pharmacol Sci* 2019;23:10354–62.